# The Electrochemical Flow Capacitor: A New Concept for Rapid Energy Storage and Recovery

*Volker Presser, Christopher R. Dennison, Jonathan Campos, Kevin W. Knehr, Emin C. Kumbur,* and Yury Gogotsi**

**Availability of grid-scale electric energy storage systems with response rates on the order of seconds plays a key role in wide implementation of renewable energy sources. Here, a new concept called the electrochemical flow capacitor (EFC) is presented. This new concept shares the major advantages of both supercapacitors and flow batteries, providing rapid charging/discharging while enabling the decoupling of the power and energy ratings. Like in supercapacitors, energy is stored in the electric double layer of charged carbon particles. A flowable carbon-electrolyte mixture is employed as the active material for capacitive energy storage, and is handled in a similar fashion to flow or semi-solid batteries (i.e., for charging/discharging, it is pumped into an electrochemical cell, and for storage, it is pumped into reservoirs). This study presents the proof-of-concept of this technology and reports initial EFC performance data obtained under static and intermittent flow operations.**

## 1. Introduction

Electrical energy storage (EES) has emerged as a key technological challenge impeding the widespread implementation of intermittent renewable energy sources such as wind and solar. Viable EES technologies are also essential for increasing grid efficiency through implementation of load-leveling and peak-shaving strategies to manage the rapid fluctuations in energy demand during the day.[1] Rapid energy recovery is also critically important to enable immediate and continuous utilization of fluctuating renewable energy sources. These critical challenges can only be met by highly efficient storage technologies that are able to quickly respond to the large and rapid fluctuations, which are inherent to electrical energy generation and demand. Despite widespread efforts and a few promising approaches, no viable EES technology exists that can efficiently manage the rapid time-shifting of energy to periods of maximum demand, at scales ranging from single-family homes to metropolitan electrical distribution installations.

Significant breakthroughs in electrical energy storage have been made within the last two decades in the fields of batteries[2] and supercapacitors.[3] However, these advances primarily address small-scale storage, such as consumer and microelectronics. Flowable electrochemical systems such as redox flow batteries (RFBs),[4] molten salt batteries (primarily Na-S),[5] or the recently reported semisolid lithium flow cell (SSFC),[6] are alternative technologies for grid-scale energy storage. Unlike traditional batteries, the unique aspect of these systems is the decoupling of energy and power ratings; such that the energy storage capacity is determined by the size of the electrolyte reservoirs, whereas the power range is dependent on the size of the electrochemical cell stack (i.e., size and quantity of individual cells) and the electrochemical processes during charge/discharge. While the decoupled power and energy storage feature allows these systems to be scaled to different energy storage applications, the major inherent issue with these technologies is that they suffer from slow charging (on the order of hours) and limited cycle lifetimes (<20 000 cycles), which hinders their widespread usage.[7]

In contrast to batteries, supercapacitors show great promise to address load-leveling, peak-shaving and grid stabilization issues as they exhibit rapid charge/discharge characteristics because energy is stored physically by ion adsorption in the electric double layer (EDL), and not through inherently slower Faradaic processes. When compared to Li-ion batteries, supercapacitors provide ~10× higher power-density, ~100× faster charge/discharge rates, and ~1000× longer lifetimes at a potentially lower cost. However, current supercapacitor technology suffers from low energy density (~20× lower than batteries) and high cost, which limits their ubiquitous implementation for smart grid applications.[8]

Here, we introduce a new dynamic energy storage concept called the "electrochemical flow capacitor" (EFC), which shows promise for use in grid-scale electrical energy storage. This concept is expected to benefit from the major advantages of both supercapacitors and flow batteries; namely the high power density and long cycle lifetime of supercapacitors and the scalable energy capacity of flow batteries. The unique

Dr. V. Presser, J. Campos, Prof. Y. Gogotsi
A. J. Drexel Nanotechnology Institute
Department of Materials Science and Engineering
Drexel University
Philadelphia, PA 19104, USA
E-mail: gogotsi@drexel.edu
C. R. Dennison, K. W. Knehr, Prof. E. C. Kumbur
Electrochemical Energy Systems Laboratory
Department of Mechanical Engineering
Drexel University
Philadelphia, PA 19104, USA
E-mail: eck32@drexel.edu

**DOI: 10.1002/aenm.201100768**

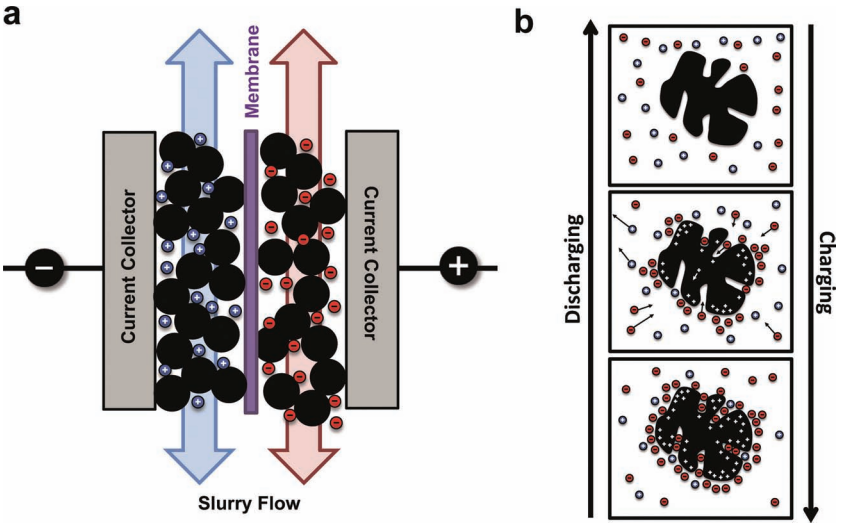


**Figure 1.** Concept of the charge storage mechanism of the electrochemical flow capacitor (EFC). A carbon/electrolyte mixture (slurry) is pumped between two polarized current collectors for charging and discharging (a). Energy is stored in the electric double layer (EDL): ions from the electrolyte counterbalance the surface charges of the polarized carbon particles (b). Discharge is accomplished by depolarizing the EDL.

aspect of this new concept is the use of a flowable carbon-electrolyte slurry for capacitive energy storage. Fundamentally, the EFC is based on the same charge storage mechanism as supercapacitors, where reversible polarization leads to the formation of the EDL by counterbalancing the surface charges of porous electrodes (**Figure 1**). As such, the operation of an EFC occurs in a way that uncharged slurry (in this case, a flowable mixture of porous carbon particles with aqueous or organic electrolyte similar to the 'slurry electrode' introduced by Kastening et al.[9]) is pumped through a polarized flow cell, where energy storage occurs through the formation of the EDL at the surface of the carbon particles. Positively charged solid particles in the slurry attract negatively charged ions for charge balancing (and vice versa). Ion diffusion from one slurry electrode to another occurs through an ion-permeable membrane that acts as an electrical insulator (Figure 1). Once charged, the slurry is pumped into an external reservoir for storage and when it is necessary to recover the stored energy, the charged slurry is again pumped through a flow cell (**Figure 2**). Charging can occur very rapidly, yet power output and energy storage are decoupled, which enables energy capacity, overcoming the major limitation of supercapacitors: the moderate amount of stored energy.

At a system level, EFCs utilize an architecture similar to that found in flow batteries.[6] The system consists of an electrochemical flow cell for charging and/or discharging, which is connected to an external circulatory system of pumps and reservoirs. Various conceptual designs of the EFC are possible and the most basic one is shown in Figure 2. A more versatile embodiment would be a double cell-stack, closed-loop system enabling charging of uncharged and discharging of previously charged slurry at the same time. This feature is of particular importance to simultaneously respond to fast fluctuations in energy production and energy consumption, which are two inherently independent parameters. Each half-cell uses a flow field or channel to direct the flow of active material over the surface of a polarized current collector.

In this study, we present the proof-of-concept of this technology and report initial performance data obtained from a prototype EFC system. Several flowable capacitive slurry compositions are benchmarked using electrochemical characterization and rheometric techniques. Both static cell and intermittent flow operation are studied. The prototype EFC shows promising performance comparable to other emerging and existing technologies, indicating that much higher performance will be possible after system optimization.

## 2. Results

### 2.1. Design of Electrochemical Flow Capacitor (EFC) Prototype

The design of the flow capacitor cell is critically important to facilitate the flow of the capacitive slurry (i.e., mitigate clogging) and maximize system performance. In particular, the flow cell design is highly dependent on the properties of the slurry used

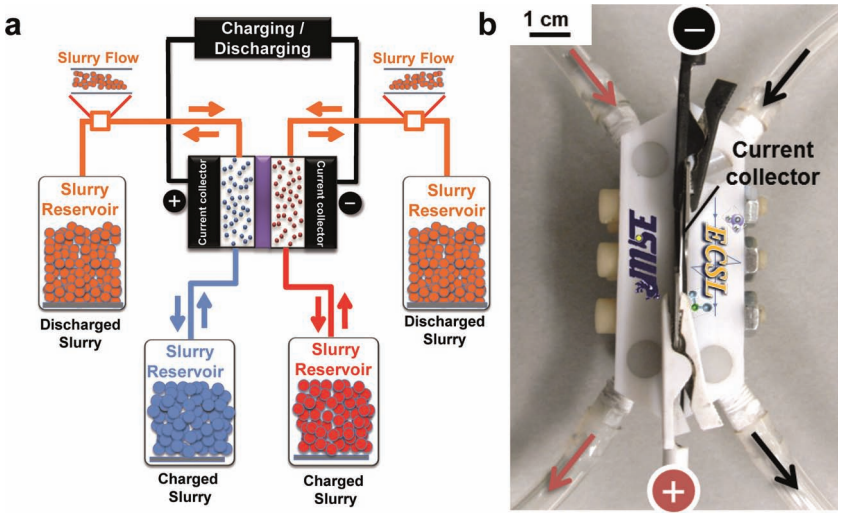


**Figure 2.** EFC system architecture. Schematic of a simple single-cell EFC, similar to the setup used in this study. Charged and discharged slurries are stored in separate containers, the size of which is determined by the energy requirements of the system (a). The EFC prototype used in this study allows intermittent flow of a carbon slurry inside an electrochemical cell for charging/discharging (b).

for capacitive storage. Several designs were considered, tested, and evaluated before selecting the reported cell design (Figure 2). The chosen cell design provided the high level of flow control required for prototype benchmarking and also enabled testing of operation modes similar to the ones which are anticipated to be encountered for a large scale EFC device. In the selected design, a single flow channel with a depth of 1.6 mm ran through each half-cell, similar to the cell described in reference.[6] Half-cells consisted of a stainless steel current collector recessed in a polytetrafluoroethylene (PTFE) flow manifold. Polymer membranes typically used in supercapacitors and batteries were used as the isolative separator between the two half-cells. Valves with a cross-sectional diameter similar to the flow channel were installed at the inlet and outlet of the cell to minimize clogging and provide physical/electrical confinement of the slurry within the cell.

### 2.2. Carbon Slurry Composition

The composition of the carbon slurry determines its rheological and electrochemical properties. In particular, the concentration of carbon particles, particle size/shape, and carrier-fluid (electrolyte) viscosity have a significant effect on the performance of the carbon slurry, and can be altered to obtain improvements in rheological and electrochemical properties for enhanced slurry flow and EFC performance. In this study, carbon slurries based on spherical porous carbons with a high surface area were tested. In a suspension, spherical carbon beads with a narrow particle size distribution provide rheological advantages, minimizing the flow-induced particle size segregation and clogging such that a smooth flow pattern can be achieved. We have tested phenolic-resin-derived activated carbon beads with average particle sizes of 161 µm (CB01), 315 µm (CB03), and 383 µm (CB02; see also Supporting Information (SI)) and non-spherical carbide-derived carbon powder obtained from a titanium carbide precursor (TiC-CDC; average particle size ~2 µm). Slurries of these porous carbons were prepared with 1 M $Na_2SO_4$ in water and 1.25 M TEA-$BF_4$ in propylene carbonate (PC). Microparticulate TiC-CDC was analyzed to enable comparison of the tested slurries against a material with a high intrinsic capacitance. X-ray microtomography shows that for a 3:1 mixture (electrolyte:carbon by mass) of CB01 resting in a 1 mm capillary, most carbon beads are in direct physical contact, creating a conductive 3D network (i.e., high bead connectivity) that enables electron transport within the active material. By increasing the electrolyte mass ratio from 3:1 to 4:1, the slurry was observed to exhibit improved macroscopic flowability with glycerol-like characteristics (**Figure 3**d). Rheological analysis indicates that with increased shear rate, a continuous decrease in the viscosity of the slurry occurs (i.e., shear-thinning) and a change in the flow characteristics of the slurry was observed (Figure 3e). A similar trend was observed for the suspension described in reference [6].

### 2.3. Electrochemical Flow Capacitor Performance

Slurries based on carbon beads (3:1 mixture) and CDC (6:1 mixture) showed pronounced capacitive behavior when charged to

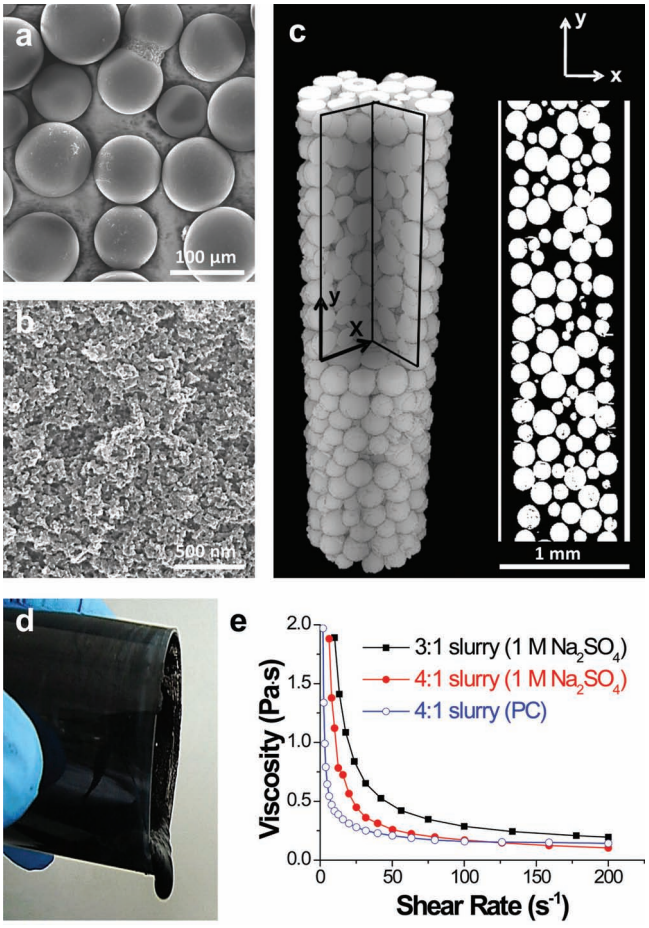


**Figure 3.** Carbon beads derived from a phenolic resin can be used as the solid component of a flowable carbon slurry due to their spherical shape. SEM shows the spherical form of CB01 carbon beads (a) while high-resolution SEM imaging reveals the porosity of the activated carbon (b). A 3:1 electrolyte:carbon mixture yields a high level of particle-particle contact as seen from X-ray microtomography (c). Flowability is improved for a 4:1 mixture (d). Rheometry shows shear-thinning related to phase separation of both the 3:1 and 4:1 liquid-solid mixture (CB01) at 25 °C in aqueous electrolyte and propylene carbonate (e).

0.6 V in 1 M $Na_2SO_4$ (aqueous electrolyte) (**Figure 4**a) and 2.7 V in 1.25 M TEA-$BF_4$ in PC (organic electrolyte) using a static laboratory cell. The organic electrolyte exhibited a lower specific capacitance for CB01 (44 F/g at 2 mV/s) when compared to the performance of CB01 in aqueous electrolyte (95 F/g at 2 mV/s; Figure 4b). TiC-CDC in aqueous electrolyte demonstrated the highest capacitance with 109 F/g at 2 mV/s, while the CB03 beads demonstrated the lowest capacitance (69 F/g) under the same conditions. The measured specific capacitance of the carbon slurries translates into an energy density of approximately 0.3 Wh/liter for the aqueous carbon slurries (e.g., comparable to the potential energy of water at 100 m height difference used for hydropower) and 3.7 Wh/liter of the PC-based carbon slurry, close to the values for commercial packed supercapacitor cells. Since the carbon weight accounts for about 30% of the total mass of the packaged commercial supercapacitors, a factor of 3–4 is

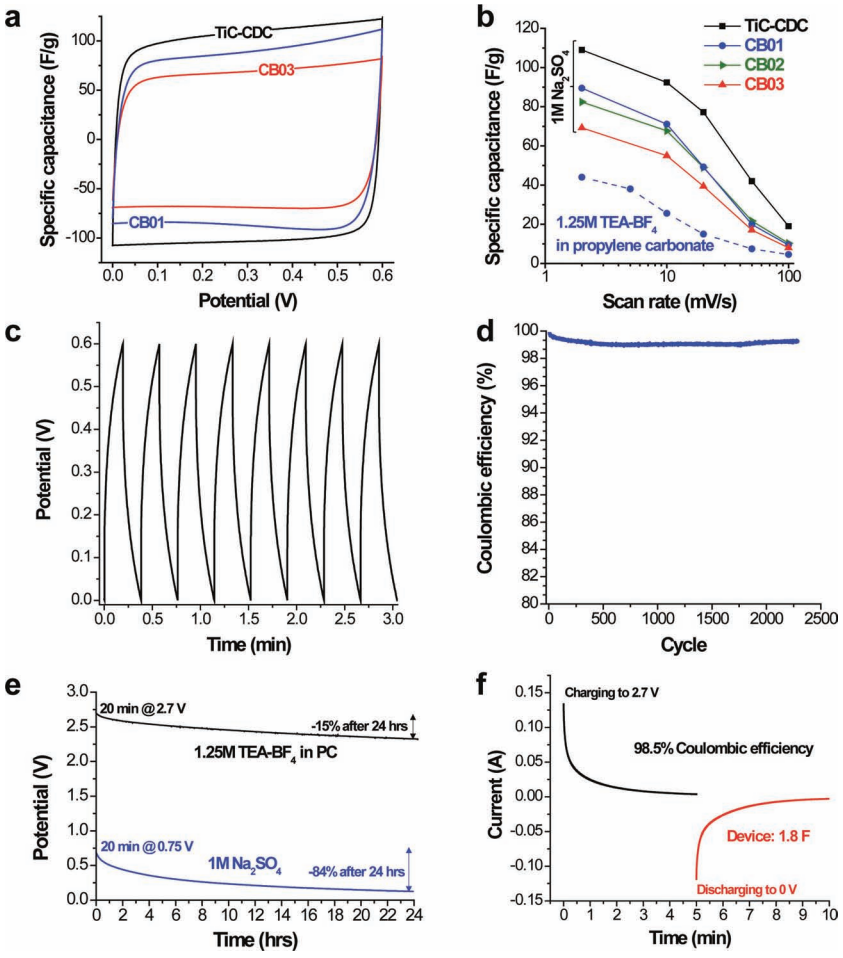


**Figure 4.** Electrochemical performance of aqueous and organic carbon slurries in a static laboratory cell. Carbon beads and TiC-CDC slurries (in 1 M $Na_2SO_4$) charged to 0.6 V at 2 mV/s show capacitive behavior as demonstrated by rectangular CVs (a). Dependency of the specific capacitance on the charge/discharge rate in aqueous and organic electrolytes (b). Galvanostatic charge/discharge (100 mA/g) of CB01 in 1 M $Na_2SO_4$ shows an ohmic drop of 4.2 $\Omega cm^2$ with no electrochemical side-reactions (c), facilitating a high coulombic efficiency of approximately 99% over 2,250 charge and discharge cycles (d). Open circuit voltage of a 3:1 CB01 slurry after charging to 0.75 V in 1 M $Na_2SO_4$ and to 2.7 V in 1.25 M TEA-$BF_4$ in PC for 20 min, respectively, shows faster voltage loss over time for the aqueous than for the organic electrolyte (e). Chronoamperometry shows an equilibrium capacitance of 49 F/g for CB01 tested in organic electrolyte and a high coulombic efficiency of >98% when charged to a cell potential of 2.7 V and subsequently discharged to 0 V.

frequently used to extrapolate the energy/power of the device from the performance of the material. However, this extrapolation is only valid for electrodes with the thickness and weight loading similar to that of commercial electrodes using 100–200 µm of carbon film on a current collector. For an EFC, for which the mass of the current collectors, separator, and other materials is small relative to the mass of the slurry, the total energy density of the system is roughly equal to that of the slurry. Thus, even a non-optimized system shows a respectable energy density in these preliminary tests. Values of up to ~7 Wh/liter can be achieved for ionic liquid electrolytes with a 4 V stability window,[10] assuming a moderate capacitance of ~40 F/g.

All studied carbons showed a moderate equivalent series resistance (ESR) of ~4 $\Omega cm^2$ when used in a toothpaste-like flowable 3:1 mass ratio of carbon in 1 M $Na_2SO_4$. This value increased by a factor of 2.7 when increasing the channel depth of the flow cell from 0.8 to 1.6 mm. The rate-performance of the carbon slurries remained limited, with significant losses in specific capacitance at scan rates faster than 10 mV/s (Figure 4b). Nonetheless, even a relatively low current density of 0.35 A/g enabled 8 full galvanostatic charge and discharge cycles within a 3 minute period (2.6 cycles per minute - one cycle every 23 seconds; Figure 4c). The corresponding gravimetric capacitance from galvanostatic charge/discharge was observed to be similar to the values obtained from cyclic voltammetry (CB01: 91 F/g in aqueous and 45 F/g in organic electrolyte). Moreover, the galvanostatic cycling performance was found to be stable, with cycle efficiencies greater than 99% for the first 2250 charge/discharge cycles (Figure 4d).

The time-dependent loss of the open circuit cell potential (referred to as self-discharge)—a common phenomenon in supercapacitors—was found to be higher for aqueous slurries than for organic carbon slurries (Figure 4e). For 20 min of charging to maximum cell potential (0.75 V for aqueous and 2.7 V for organic electrolyte), the open circuit voltage dropped to 16% of the initial voltage (0.75 V) after 24 hrs for 1 M $Na_2SO_4$ aqueous electrolyte, but remained at a high level of 2.3 V (= 85%) for the organic electrolyte. The latter, while being a faster decay than observed in optimized commercial packed cells, is still in the range of values reported for supercapacitors.[11] We note that charging for a longer period will further decrease the loss of potential over time,[11b] and the separate storage of the positively and negatively polarized slurries is expected to further decrease self-discharge by eliminating leakage current, which is associated with the (undesired) charge transfer across the porous separator and insulating gaskets.

In terms of specific capacitance, both cyclic voltammetry and galvanostatic charge/discharge yield a specific capacitance which is rate-dependent (i.e., depends on scan rate or current density). This can be attributed to the dynamic effects associated with transport resistance inside micro- and mesopores of the carbon particles, and across the separator. As found by chronoamperometry (Figure 4f), the intrinsic equilibrium capacitance of CB01 (aqueous: 125 F/g, organic: 49 F/g) is comparable, yet higher than the capacitance derived from rate-dependent methods (aqueous: +37%, organic: +9%; see SI for more detailed discussion). When compensating for the leakage current, the coulombic efficiency ($\varepsilon_c$) of the EFC prototype was observed to be 98.5%, which is in a very good agreement with the coulombic efficiency derived from galvanostatic charge/discharge (≈99%).

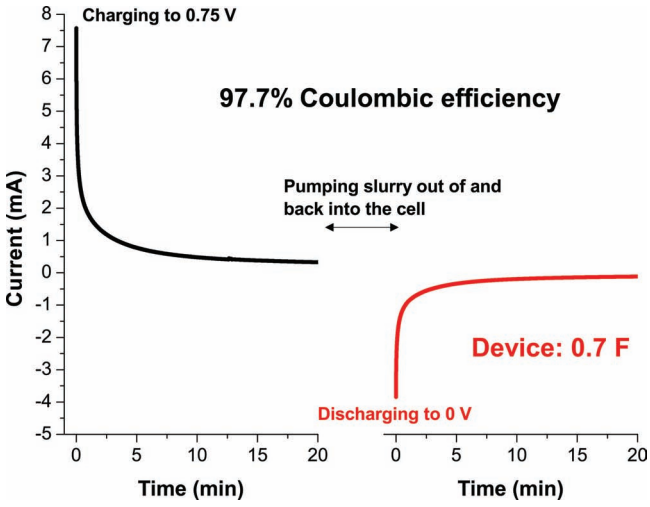


**Figure 5.** Electrochemical performance in intermittent flow mode. After being charged at a potential of 0.75 V for 20 min, a carbon slurry based on a mixture of CB01 and 1 M $Na_2SO_4$ is completely removed from the electrochemical cell and then pumped back into the cell to be discharged at 0 V for 20 min. When compensating for the leakage current, this translates into a coulombic efficiency of ~98% and a device capacitance of 0.7 F. We note that this device capacitance is lower than the static cell because of the higher electrolyte:carbon ratio (4:1 instead of 3:1), which helped promote flowability.

In order to evaluate the dynamic energy storage ability of the electrochemical flow capacitor, carbon slurry CB01 based on the aqueous electrolyte was tested in an intermittent-flow configuration. The main goal of this test was to verify that initially charged carbon particles maintain their charge after hydraulic handling. The voltage efficiency ($\varepsilon_V$) was observed to reach 55.7%, while the coulombic efficiency was around 97.7% (**Figure 5**). The low voltage efficiency can be attributed to the significant voltage drop during the time in which the slurry rests outside the electrochemical cell. As mentioned before, we note that the voltage drop over time is a widely observed phenomenon in static supercapacitors and has two main components: (1) unwanted charge exchange between the opposing half-cells (charge recombination), which results in a loss of stored charge and a decrease in cell potential, and (2) ion redistribution within pores of carbon particles, which only results in a decrease of cell potential. One important distinction is that the potential drop in the EFC is not associated with a significant loss of the stored charge, as indicated by the high coulombic efficiency. This indicates that the potential drop is mainly caused by ion redistribution[11a] during the time the slurry rests outside the electrochemical cell, rather than charge recombination. We note that while the leakage current for our prototype cell can be up to 44% of the total charge, it can be significantly minimized through further optimization of the cell design.

## 3. Discussion

The design of the flow capacitor cell and the flow channel in particular, play a critical role in the performance of the EFC. In order to minimize ohmic losses, it is generally advantageous to use a very shallow channel geometry, which allows free passage of the slurry without clogging. The overall length of the channel determines the charging rate and the residence time of the slurry within the cell. While a simple channel of constant cross-section was used in this study, it is foreseeable that more elaborate channel designs will yield improved system performance. In particular, multiplexing will enable large quantities of carbon slurry to be charged or discharged in parallel to accommodate the storage or recovery of large amounts of energy. In addition, it is possible to lower the contact resistance and achieve higher flow rate capability through further engineering of the current collectors.

As seen in this proof-of-concept study, the observed capacitance of carbon beads (up to 125 F/g in aqueous electrolytes) is comparable to what has been reported for activated carbons in $Na_2SO_4$ (~120 F/g)[12] or phenolic-resin-derived carbon spheres (>150 F/g).[13] We expect a further increase in the intrinsic carbon capacitance (>200 F/g) when utilizing materials such as ordered mesoporous carbons[14] or hydrothermally carbonized activated carbons.[15] While the energy density—one of the most important metrics of energy storage systems—scales linearly with the capacitance, it has a quadratic dependence on the cell potential (i.e., $E = 0.5\ CV^2$). This means that even for a moderate capacitance, a comparatively high energy density can be reached in electrolytes, such as ionic liquids, which enable operation in a large voltage window. In addition, eutectic ionic liquid mixtures have recently been shown to enable supercapacitor usage in a very broad temperature window (–50 to +100 °C)[16] where a grid-scale EFC may be required to operate. Non-volatility in conjunction with a wide usable voltage window makes ionic liquids a particularly attractive electrolyte for the electrochemical flow capacitor concept, especially if their production volume increases with a decrease in cost. Very low operation temperatures are not limited to ionic liquids but are also possible when employing organic electrolytes. It has been shown recently that temperatures as low as –70 °C are possible when employing spiro-(1,1′)-bipyrrolidinium tetrafluoroborate (SBP-$BF_4$) in a 1:1 (vol%) mixture of acetonitrile and methyl formate which can be considered as an alternative electrolyte to ionic liquids.[17]

It is clear that a low interparticle connectivity will negatively affect the rate-performance and the charge transfer efficiency of carbon slurries. This aspect can be addressed by optimizing the size and loading of the carbon beads, but there should be a balance of flowability (best with low solid/liquid ratios) and charge transfer efficiency (best with high solid/liquid ratios). While a narrow particle size distribution is desirable to avoid granular convection, the flowability and particle contact would both directly benefit through the use of smaller carbon beads. To date, carbon microspheres with different sizes can be obtained from various chemical syntheses.[18] For example, spherical carbon particles with the size of a few micrometers can be obtained by hydrothermal synthesis,[19] while submicrometer-sized mesoporous carbon spheres can be obtained by template synthesis.[20] Pseudocapacitive carbon microspheres (≤1 μm) produced by ultrasonic spray pyrolysis have been shown to yield a very high capacitance of up to 341 F/g.[21] Such carbon materials possess potential to improve the energy density of the

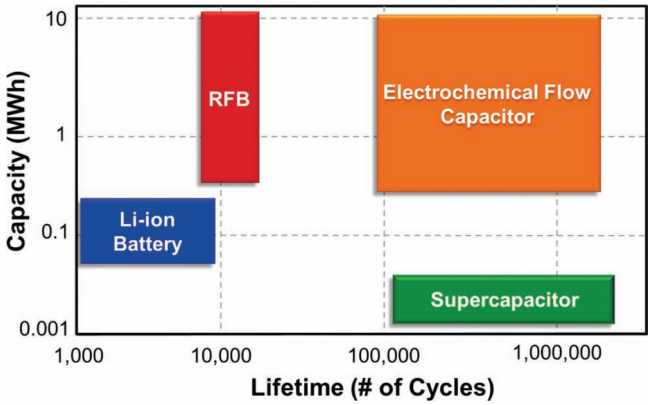


**Figure 6.** Comparison of the EFC and other EES technologies. The EFC is expected to combine the high cycle lifetime of supercapacitors with the scalability and system energy rating of conventional redox flow batteries, addressing a critical gap in current EES technologies.

EFC, and therefore are potential candidates for use as an active material.

Self-discharge is a chronic problem for supercapacitors, and the voltage loss over time is higher for supercapacitors compared to batteries.[11b] The EFC prototype studied herein exhibits self-discharge and voltage loss rates comparable to the values reported for conventional supercapacitors when the slurry remains confined inside the charge/discharge cell. A lower self-discharge is expected to be achieved for carbons with optimized pore structures, and when separately storing the negatively- and positively-charged slurries. The separate storage of charged carbon slurry will not influence the phenomenon of charge/ion redistribution, but is expected to minimize the actual self-discharge through elimination of the cross-separator leakage current. Studies are underway to provide metrics for the long-term behavior of resting polarized slurries.

The EFC represents a new conceptual approach to electrical energy storage system design, and it is expected to complement existing EES technologies (**Figure 6**). Like supercapacitors, EFCs are expected to show a very long cycle lifetime as the operation only involves fully reversible polarization of the electrolyte, without Faradaic side-reactions, which can be detrimental to the device lifetime. However, on an energy-rating level the EFC overcomes the capacity limitations of conventional static supercapacitors through decoupled energy storage and recovery, since energy simply scales with the size of the reservoirs used to hold charged capacitive slurry. Moreover, by exploiting the principle of multiplexing, the response rate can be tailored by varying the number of active charging/discharging channels. The architectural similarities between RFB and the EFC imply that similar energy capacities should be possible. In addition, this new concept eliminates the need for additional current collectors, separators and packaging used in supercapacitors, and, therefore, makes it possible to decrease EES cost as compared to conventional supercapacitor cells.

In summary, the EFC concept shows promise as a stationary energy storage system. In this study, we demonstrate the proof-of-concept, and provide initial performance data for a non-optimized system under static and intermittent flow conditions. With further development, it is expected that the EFC will approach the power density and lifetime of conventional electrochemical capacitors, combined with the scalability of flow batteries. Specific areas for optimization include slurry composition, in terms of electrolyte, solid loading, active materials, etc., and flow cell design, in terms of channel geometry and cell operation. Along with the molten salt battery, redox flow battery, and semi-solid battery technologies, the electrochemical flow capacitor may help to improve grid efficiency and accelerate widespread implementation of renewable energy sources.

## 4. Experimental Section

*Materials*: Carbon beads (referred to as CB) derived from phenolic resin were obtained from MAST carbon (United Kingdom) and Antoxineer (People's Republic of China). MAST 125-250 (CB01; average particle size: 161 ± 35 μm) and MAST 250-500 (CB02; average particle size: 385 ± 53 μm) carbon beads had an average volume-weighted pore size of 8.6 nm and a BET surface area of 1341 $m^2/g$. Antoxineer spherical active carbon granules (CB03) had an average particle size of 315 ± 49 μm with an average volume-weighted pore size of 1.2 nm, and a BET surface area of 1569 $m^2/g$. TiC-CDC was obtained from dry chlorination of TiC[22] with a particle size of 2 μm from Alfa Aesar (Stock # 40178) at 1000 °C for 6 h, with subsequent annealing in hydrogen at 600 °C for 3 h. The particle size remained unchanged after chlorination.[22] The volume-weighted average pore size was 1.1 nm and the BET surface area 1815 $m^2/g$. For more information see SI.

$N_2$ gas sorption was carried out in a Quadrasorb gas sorption instrument (Quantachrome, USA) and the average, volume-weighted pore size was derived from the cumulative pore volume assuming slit-shaped pores and using the quenched-solid density functional theory (QSDFT) algorithm. The pore size distributions are provided in the SI.

A Zeiss Supra 50VP scanning electron microscope (Carl Zeiss AG, Germany) operating at 3 kV was used for electron microscopy. A Skyscan 1172 (Skyscan US Inc., USA) was used for X-ray microtomography (voxel resolution: $1.92^3$ $\mu m^3$). Viscosity was measured using a TA Instruments (USA) AR rheometer in a rotational concentric cylinder geometry at room temperature.

Slurry preparation was accomplished by mixing carbon beads or CDC particles with carbon black (100% compressed; Alfa Aesar, USA) to achieve a 9:1 weight ratio. The carbon black was used as a conductive additive. An appropriate amount of electrolyte (either 1 M $Na_2SO_4$ in water or 1.25 M TEA-$BF_4$ in propylene carbonate) was added to achieve the desired electrolyte-carbon ratio.

*Electrochemical measurements*: All measurements were carried out at ambient temperature with a VMP3 or SP150 potentiostat/galvanostat (BioLogic, France). Experiments in aqueous electrolyte were conducted in air and the organic electrolyte testing was carried out in an argon-filled glove box.

Cyclic voltammetry was carried out at 2, 5, 10, 20, 50, and 100 mV/s scan rates for a voltage window of 0.60 and 0.75 V (aqueous), and 2.7 V (PC). From cyclic voltammetry, the capacitance is derived using the equation (1):

$$C_{sp} = \frac{\frac{2}{\Delta E v} \cdot \int i dV}{m}, \quad (1)$$

where $\Delta E$ is the voltage window, $i$ is the discharge current, $V$ is the voltage, $v$ is the scan rate, and $m$ is the mass of carbon in one electrode. The factor of 2 accounts for the two electrode setup, where the charge is evenly distributed between two capacitors in series.[23] We note that the y-axis (F/g) in Figure 4a-b was calculated by dividing twice the measured current by the scan rate and normalizing it by the weight of one electrode (corresponding to $m$, as defined above).

Galvanostatic charge/discharge was conducted at 100 mA for 0.6 V (aqueous) and 2.7 V (organic) windows, with charge times of 120 s. The series resistance was calculated from the ohmic drop observed at the start of the discharge cycle, and the capacitance was derived from the slope of the discharge curves. All values for the capacitance were normalized by the weight of the carbon material, not the total slurry mass, to enable a direct comparison with conventional supercapacitor electrodes (which are also normalized to the content of active material). The specific capacitance $C_{sp}$ was calculated from galvanostatic cycling using Equation (2):

$$C_{sp} = \frac{2i}{m \cdot \left(\frac{dV}{dt}\right)}, \quad (2)$$

where $dV/dt$ is the slope of the discharge curve.

Equilibrium capacitance was extracted from chronoamperometry.[24] After a 30 min discharge period (at 0 V), the cell was charged to a certain cell potential (e.g., 2.7 V) for 5 min and then discharged to 0 V for 5 min. While the current that was measured during charging was superimposed by the leakage current of the system, integration of the discharge curve directly yielded the charge of the two-electrode setup. The capacitance was extracted from the discharge curves with Equation (3) (see also SI)

$$C_{sp} = \frac{\frac{2}{\Delta E} \cdot \int i dt}{m} \quad (3)$$

The EFC prototype (Figure 2b) consisted of two stainless steel current collectors recessed in PTFE flow manifolds. 6 mm diameter throughputs allowed slurry to flow into and out of the charge/discharge cell with a $38 \times 6$ mm$^2$ active area (per half-cell). Two 1600 µm thick PTFE gaskets provided lateral confinement of the slurry and a polyvinylidene fluoride (PVDF) membrane with a mesh width of 100 nm (Durapore; Merck Millipore, Germany) served as a separator. Six nylon screws along the length of the cell ensured sealing of the enclosed carbon slurry during charge/discharge and flow operations.

Prior to intermittent-flow testing, slurry was pumped into the EFC prototype *via* a syringe. The cell then underwent 20 cyclic voltammetry cycles from 0–0.75 V at 10 mV/s to precondition the slurry and to ensure that the internal pore-space was ion-accessible. The cell was then held potentiostatically at 0 V to dissipate any remaining charge, then charged potentiostatically at 0.75 V for 20 min. At the end of the charging period, the charged slurry was withdrawn from the cell using a syringe. The slurry was then returned to the cell and discharged potentiostatically at 0 V for 20 min. The resulting chronoamperometric profile was then analyzed to determine the voltage and coulombic efficiencies of the system. Voltage efficiency ($\varepsilon_V$) was calculated using Equation (4):

$$\varepsilon_V = \frac{V^{max}_{discharge}}{V^{min}_{charge}} \cdot 100\% \quad (4)$$

The coulombic efficiency ($\varepsilon_C$; also referred to as Faradaic or current efficiency) was determined according to Equation (5) and corrected for leakage current:

$$\varepsilon_C = \left| \frac{\int I_{discharge} dt}{\int I_{charge} dt} \right| \cdot 100\% \quad (5)$$

## Supporting Information

Supporting Information is available from the Wiley Online Library or from the author.

## Acknowledgements

The authors would like to thank C. R. Perez for help with sample preparation and electrochemical measurements, K. Jost for helpful discussions and proof-reading, and B. Dyatkin for assistance with gas sorption measurements (all Drexel University). The authors would also like to thank M. Heon and A. Pentecost (Drexel University) for SEM measurements, which were carried out using instruments in the Centralized Research Facility (CRF) of the College of Engineering, Drexel University. Dr. P. M. Biesheuvel (Wageningen University) is gratefully acknowledged for bringing chronoamperometry to the attention of the authors and for valuable discussions. The assistance of G. R. Klinzing (Drexel University) with X-ray microtomography is gratefully acknowledged. The authors would like to thank J. J. Biel-Goebel (Drexel University) for helpful discussions on cell design and assistance with cell sealing. V.P. and Y.G. were supported as part of the Fluid Interface Reactions, Structures and Transport (FIRST) Center, an Energy Frontier Research Center funded by the US Department of Energy, Office of Science, Office of Basic Energy Sciences under award no. ERKCC61. V.P. also acknowledges financial support by the Alexander von Humboldt Foundation. C.R.D. was supported by the US National Science Foundation Integrated Graduate Education and Research Traineeship (IGERT) in Nanoscale Science and Engineering under Grant No. DGE-0654313. K.W.K. gratefully acknowledges the support of the NSF REU program (Grant No: 235638), and E.C.K. gratefully acknowledges the support of the Southern Pennsylvania Ben Franklin Energy Commercialization Institute (Grant No: 001389-002). J.C. was supported by the US National Science Foundation Bridge to the Doctorate Fellowship Program (Grant No: 1026641).

Received: December 20, 2011
Revised: March 7, 2012
Published online: May 23, 2012

[1] Z. Yang, J. Zhang, M. C. W. Kintner-Meyer, X. Lu, D. Choi, J. P. Lemmon, J. Liu, *Chem. Rev.* **2011**, *111*, 3577.
[2] a) P. G. Bruce, B. Scrosati, J.-M. Tarascon, *Angew. Chem. Int. Ed.* **2008**, *47*, 2930; b) M. Armand, J. M. Tarascon, *Nature* **2008**, *451*, 652; c) J. W. Long, B. Dunn, D. R. Rolison, H. S. White, *Chem. Rev.* **2004**, *104*, 4463.
[3] a) P. Simon, Y. Gogotsi, *Nat. Mater.* **2008**, *7*, 845; b) T. Brezesinski, J. Wang, S. H. Tolbert, B. Dunn, *Nat. Mater.* **2010**, *9*, 146; c) W. G. Pell, B. E. Conway, *J. Power Sources* **2001**, *96*, 57.
[4] T. Nguyen, R. F. Savinell, *Electrochem. Soc.Interface* **2010**, *19*, 54.
[5] T. Oshima, M. Kajita, A. Okuno, *Int. J. Appl. Ceram. Technol.* **2004**, *1*, 269.
[6] a) Y.-M. Chiang, W. C. Carter, B. H. Ho, M. Duduta, US 2010/0047671 Patent, **2009**; b) M. Duduta, B. Ho, V. C. Wood, P. Limthongkul, V. E. Brunini, W. Craig Carter, Y.-M. Chiang, *Adv. Energy Mater.* **2011**, *1*, 511.
[7] M. Skyllas-Kazacos, M. H. Chakrabarti, S. A. Hajimolana, F. S. Mjalli, M. Saleem, *J. Electrochem. Soc.* **2011**, *158*, R55.
[8] J. R. Miller, A. F. Burke, *Electrochem. Soc. Interface* **2010**, *17*, 53.
[9] B. Kastening, T. Boinowitz, M. Heins, *J. Appl. Electrochem.* **1997**, *27*, 147.
[10] A. Izadi-Najafabadi, S. Yasuda, K. Kobashi, T. Yamada, D. N. Futaba, H. Hatori, M. Yumura, S. Iijima, K. Hata, *Adv. Mater.* **2010**, *22*, E235.
[11] a) M. Kaus, J. Kowal, D. U. Sauer, *Electrochim. Acta* **2010**, *55*, 7516; b) J. Kowal, E. Avaroglu, F. Chamekh, A. Senfelds, T. Thien, D. Wijaya, D. U. Sauer, *J. Power Sources* **2009**, *196*, 573.
[12] Q. T. Qu, B. Wang, L. C. Yang, Y. Shi, S. Tian, Y. P. Wu, *Electrochem. Commun.* **2008**, *10*, 1652.
[13] S.-I. Lee, S. Mitani, C. W. Park, S.-H. Yoon, Y. Korai, I. Mochida, *J. Power Sources* **2005**, *139*, 379.
[14] M. Rose, Y. Korenblit, E. Kockrick, L. Borchardt, M. Oschatz, S. Kaskel, G. Yushin, *Small* **2011**, *7*, 1108.

[15] L. Wei, M. Sevilla, A. B. Fuertes, R. Mokaya, G. Yushin, *Adv. Energy Mater.* **2011**, *1*, 356.
[16] R. Lin, P.-L. Taberna, S. Fantini, V. Presser, C. R. Perez, F. Malbosc, N. L. Rupesinghe, K. B. K. Teo, Y. Gogotsi, P. Simon, *J. Phys. Chem. Lett.* **2011**, *2*, 2396.
[17] Y. Korenblit, A. Kajdos, W. C. West, M. C. Smart, E. J. Brandon, A. Kvit, J. Jagiello, G. Yushin, *Adv. Funct. Mater.* **2012**, 10.1002/adfm.201102573.
[18] A. A. Deshmukh, S. D. Mhlanga, N. J. Coville, *Mater. Sci. Eng.* **2010**, *70*, 1.
[19] a) B. Basavalingu, J. M. Calderon-Moreno, K. Byrappa, Y. G. Gogotsi, M. Yoshimura, *Carbon* **2001**, *39*, 1763; b) G. Li, C. Guo, C. Sun, Z. Ju, L. Yang, L. Xu, Y. Qian, *J. Phys. Chem. C* **2008**, *112*, 1896.
[20] Z. Lei, N. Christov, L. L. Zhang, X. S. Zhao, *J. Mater. Chem.* **2011**, *21*, 2274.
[21] H. Kim, M. E. Fortunato, H. Xu, J. H. Bang, K. S. Suslick, *J. Phys. Chem. C* **2011**, *115*, 20481.
[22] R. Dash, J. Chmiola, G. Yushin, Y. Gogotsi, G. Laudisio, J. Singer, J. Fischer, S. Kucheyev, *Carbon* **2006**, *44*, 2489.
[23] M. D. Stoller, R. S. Ruoff, *Energy Environ. Sci.* **2010**, *3*, 1294.
[24] D. Brogioli, R. Zhao, P. M. Biesheuvel, *Energy Environ. Sci.* **2011**, *4*, 772.